Medical Devices: Evidence and Research

Dovepress

open access to scientific and medical research

Open Access Full Text Article

ORIGINAL RESEARCH

A Cadaver-Based Biomechanical Evaluation of a Novel Posterior Approach to Sacroiliac Joint Fusion: Analysis of the Fixation and Center of the Instantaneous Axis of Rotation

Dawood Sayed[1]
Kasra Amirdelfan[2]
Ramana K Naidu[3]
Oluwatodimu R Raji[4]
Steven Falowski[5]

[1]The University of Kansas Medical Center, Kansas City, KS, USA; [2]IPM Medical Group, Walnut Creek, CA, USA; [3]California Orthopedics & Spine, Larkspur, CA, USA; [4]Medical Device Development, San Francisco, CA, USA; [5]Neurosurgical Associates of Lancaster, Lancaster, PA, USA

Purpose: The purpose of this study was to assess the stabilizing effect of a posterior joint fixation technique using a novel cortical allograft implant in unilateral and bilateral fixation constructs. We hypothesize that fixation would reduce the joint's range of motion during flexion-extension, axial rotation, and lateral bending loads. We also hypothesize that fixation would shift the center of the instantaneous axis of rotation during the predominant flexion-extension motions towards the implant's location, and that this shift would be correlated with the reduction in flexion-extension range of motion.

Materials and Methods: Six cadaveric sacroiliac joint specimens were tested under intact, unilateral fixation, and bilateral fixation conditions. The total range of motion (ROM) of the sacroiliac joint in flexion–extension, lateral bending, and axial rotation were evaluated by an optical tracking system, in a multidirectional flexibility pure moment model, between ± 7.5 Nm applied moment loads. The centers of the instantaneous axis of rotation (cIAR) of the sacroiliac joint were evaluated during flexion-extension loading. A correlation analysis was performed between the ROM reduction in flexion-extension upon implantation and shift of the cIAR to the graft implantation site.

Results: Unilateral and bilateral fixations generated sacroiliac joint ROM reductions in flexion-extension, lateral bending, and axial rotation motions. Fixation shifted the cIAR to the graft implantation site. Reduction in the total range of motion had a moderate correlation with the shift of the cIAR.

Conclusion: Our novel posterior approach presents a multifaceted mechanism for stabilizing the joint: first, by the reduction of the total range of motion in all planes of motion; second, by shifting the centers of the instantaneous axis of rotation towards the implant's location in the predominant plane of motion, ensuring little to no motion at the implantation site, thus promoting fusion in this region.

Keywords: range of motion, arthrodesis, allograft, distraction interference

Introduction

Degenerative changes in the sacroiliac joint (SIJ) account for 10% to 38% of patients reporting chronic low back pain.[1] As a result, joint fusion has been implemented as a treatment method.[2–5] Fixation techniques described in literature can be classified into lateral and posterior approaches.[2,6–17] Currently, the lateral approach is the most common approach utilized for sacroiliac joint arthrodesis, especially due to the prevalence of biomechanical and clinical studies assessing its efficacy.[2,8–13] In contrast, posterior

Correspondence: Oluwatodimu R Raji
The Taylor Collaboration Attn: Richard Raji, 450 Stanyan Street, San Francisco, CA, 94117, USA
Tel +1 510 570 7741
Email richardraji@mdevdev.com

Received: 4 November 2021
Accepted: 9 December 2021
Published: 17 December 2021

approaches remain yet to be explored biomechanically, amidst increasing interest due to their reduced potential for damage to the sacral nerves and muscles, which remains a complication of the lateral approach.[17]

One interpositional posterior approach utilizes a rectangular-shaped cortical allograft with serrations on its sides (LinQ fusion System, PainTEQ, Tampa, Florida) which is inserted posteriorly towards the anterior portion of the sacroiliac joint (Figure 1). The placement of the allograft distracts the joint to relieve stresses on the joint cartilage and ligaments, while its serrations allow for coupling of the medial and lateral portions of the joint.[2,14–18] Fusion of the joint is promoted in the region where its articulating bodies are coupled, as this region becomes the center of rotation of the joint. This induces stability at and localizes compressive forces at the implantation site where fusion is desired, while also relieving stresses on capsular neural structures and those neural structures directly anterior to the joint. Centers of rotation have previously been used to drive implant design and to assess the quality of spinal motion.[19–23]

Thus, in this study, we aimed to assess the stabilizing effect of a posterior SIJ fixation technique using a novel cortical allograft implant in unilateral and bilateral fixation constructs, within the multidirectional bending flexibility model. We hypothesize that both unilateral and bilateral fixation would reduce the joint's range of motion during flexion-extension, axial rotation, and lateral bending loads. We also hypothesize that the posterior technique would shift the center of the instantaneous axis of rotation (cIAR) during the predominant flexion-extension motions towards the implant's location and that this shift would be correlated with the reduction in flexion-extension range of motion.

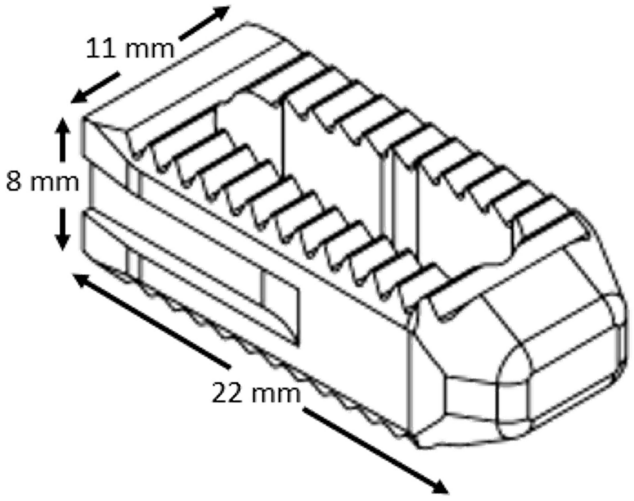

Figure 1 Illustration of the rectangular-shaped cortical allograft.

Materials and Methods

Specimen Preparation

Six fresh-frozen cadaveric joint specimens from three pelvises were obtained from the American Association of Tissue Banks (AATB) accredited tissue bank. A sample size of four sacroiliac joints was calculated using the following assumptions: standard deviation of 27%, 80% power, 0.05 level of significance, and an effect size of 50% reduction, in flexion/extension.[9] Potential specimens were screened and eliminated if there was a history of smoking, drug abuse, chemotherapy, radiation treatment, previous spine surgery, or fragility fractures. The age at the time of death ranged 35 ± 1 years, average body mass index was 26 ± 2. Dual-energy x-ray absorptiometry scans of the lumbar vertebra were used to exclude osteoporotic tissue, the average L1-L4 t-score was 0.8 ± 0.6, and the average L4 bone density was 1.3 ± 0.2 g/cm^2, female-to-male ratio was 2:1. Additionally, all specimens were screened with Computer Tomography (CT) scans to exclude donors that exhibited bony bridging/fusion of the sacroiliac joint.[24]

Each specimen was prepared by stripping away the soft tissue, with care taken not to disrupt the sacroiliac joints, sacrolumbar joint, or the pubic symphysis. Before potting, steel wires were placed through the ischium and the L4 vertebrae to allow for a better fixation of the epoxy. Each ischium was potted individually in a fast curing resin (Smooth-Cast 300Q, Smooth-On, Inc, Easton, Pennsylvania) with the superior-inferior axis, defined physiologically, aligned with gravity.[25] Wood screws were inserted through the L4 endplate and into the L5, rigidly fixing both vertebral bodies. The L4 vertebral was then potted in a cylindrical mold with fast curing resin to allow for mounting of a pure moment ring during testing (Figure 2). The custom pure moment ring was attached with fluoroscopic guidance using the pubic symphysis to align the anterior-posterior axis of the ring.

Sacral Perimeter Marking

Under fluoroscopy, the superior end of the sacral ala, the inferior end of the sacral ala (which lies adjacent to the pelvic brim of the ilium), were identified and marked using a pelvic inlet view. Meanwhile, the inferior end of the sacroiliac joint (which lies at the third sacral level) was identified and marked in anterior-posterior view (Figure 3).

Motion Calibration

To track the motion of the iliac and sacrum during biomechanical testing, an optical tracking system was utilized (3D Investigator, Northern Digital Inc., Waterloo, Ontario,

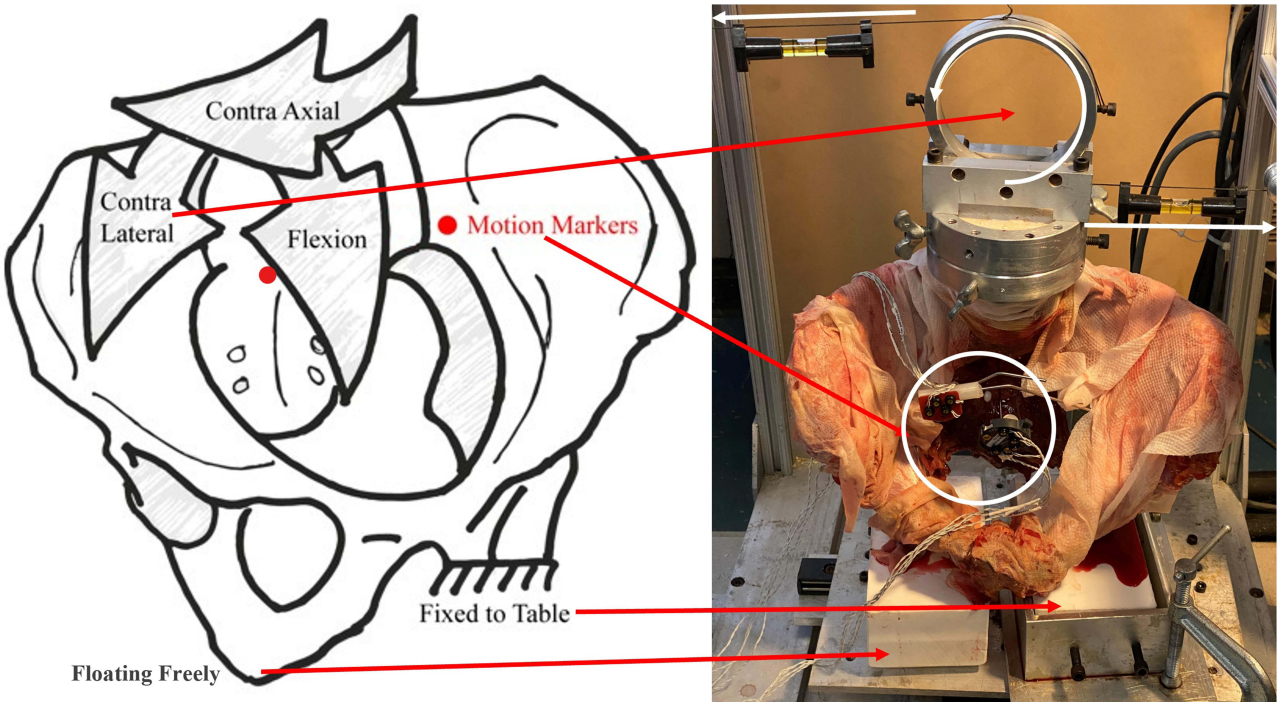

Figure 2 Illustration (left) of the biomechanical model, and picture (right) of the test setup in the left single-leg stance. Pure moments were applied to the potted lumbar spine using a moment ring system, as shown (in white). Relative motions between the sacrum and the iliac were tracked with motion markers rigidly fixed to each bone using steel pins (white). Not pictured in the illustration are counternutation, ipsi axial rotation, and ipsi lateral bending arrows. Pure moment ring system in picture, is set up for contra- (right-) lateral bending of the left sacroiliac joint.

Canada). The Optotrak 3020 optical active-marker system has been reported to have a precision of 0.02° and 0.125 mm, with repeatability limits of 0.04° and 0.15 mm.[26] Infrared markers were rigidly attached to the medial portion of each ilium and the third sacral body. To align the coordinate system of the camera to the anatomical axes of the specimen, a digital probe was used to mark various points on the specimen. The origin was defined as the most superior point of the sacral ala. Two points on the moment ring (previously aligned) were taken to orient the coordinate system to the physiological axes (superior-inferior and medial-lateral). The bottom of the sacral ala and the bottom of the sacroiliac joint were also digitally probed to align and orient the digital sketch of the sacrum to the fluoroscopic images taken during specimen preparation and fixation. These oriented marker positions were recorded for 5 s at 100 Hz during each loading interval.

Biomechanical Model

Specimens were tested using a fixed moment ring cable system. The cables were wound around the moment ring and ran through pulleys in the appropriate direction before being connected to the actuator (858 Mini Bionix II; MTS, Eden Prairie, MN, USA) to induce the desired bending movement.[27] For all testing, a single-leg stance was utilized; the joint undergoing testing was rigidly clamped to a platform mounted on linear bearings allowing transverse movement, while the untested joint was free to move (Figure 2).[8–13]

The specimens were first pre-conditioned, which consisted of three cycles of loading from 0 N-m to 7.5 N·m. The specimens were tested quasi-statically (fourth loading cycle), from 0 N·m to 7.5 N·m in 1.5 N·m increments with 45 s holds at each load. Motion tracking data was recorded at the end of each hold before ramping up to the next load level. Each specimen was loaded in six anatomical bending directions: flexion, extension, left/right lateral bending, and left/right axial rotation.[8–13] Each loading was performed under a compressive axial follower load of 15 N, due to the weight of the pure moment ring on the potted L4 vertebrae.

The specimens were first tested (on both sides) with both sacroiliac joints intact. Subsequently, fixations were performed by implanting the allograft (LinQ SI Joint Stabilization System; PainTEQ) in one (unilateral) and both (bilateral) sacroiliac joint side(s). Both ipsilateral and contralateral joints were tested in standing posture after each fixation. All fixations were performed by a board-certified interventional pain specialist. The implants were placed in a cephalad trajectory adjacent to the second sacral neural foramina (Figure 3).

Figure 3 Fixation with bone allograft implants were performed according to the manufacturer's recommended technique. Black pins in fluoroscopic images, identify the sacral perimeter.

Outcome Measurements

The primary outcomes measured are documented in Table 1. Relative rotations between the iliac and sacral coordinate systems were calculated at each loading interval. The range of motion was calculated for flexion-extension, right-left lateral bending, and right-left axial rotation for the intact and bilateral fixation schemes. The locations of the sacral markers relative to the iliac coordinate system were recorded at each loading interval and used for cIAR calculations. Centrodes of the IAR during Flexion-Extension moments were calculated between loading intervals 1.5 Nm apart, which produced an adequate amount of angular separation (~0.1°).[28] Using computer software (MATLAB 2020a, The MathWorks Inc, Natick, Massachusetts), lines were made connecting the location of each sacral perimeter marking, to its new location at each instance of loading (Table 1). Perpendicular bisectors were then extrapolated from these, and the intercept was the locus of the instantaneous axis of rotation (IAR) for that loading instance. The graft's implantation site was determined relative to the sacral markings by assessing the lateral fluoroscopic images taken during implantation in conjunction with ImageJ (ImageJ, U.S. National Institutes of Health, Bethesda, Maryland, USA).

Statistical Analysis

The total range of motion, as well as distance from the graft's implantation site to the plane center of the instantaneous axis of rotation (cIAR) in the sagittal plane, were calculated and compared between intact and each fixation scheme using paired t-tests at $p \leq 0.05$ (SAS, SAS Institute, Cary, North Carolina, United States). Correlation analysis was also performed between the percent reduction in total range of motion during flexion-extension loads, and the distance the cIAR moved towards the allograft's implantation site upon fixation. k-means of bilateral fixed joint clusters were utilized in conjunction with unilateral fixation data for correlation analysis (SAS, SAS Institute, Cary, North Carolina, United States). All data are reported as mean ± one standard deviation unless otherwise stated.

Results

The range of motion (ROM) results are shown in Figure 4. Flexion/extension loading produced the largest total range of motion, followed by axial rotation, and lateral bending. During flexion/extension loading, unilateral and bilateral sacroiliac joint fixations, respectively, resulted in a 34% ± 27% ($p = 0.049$) and 39% ± 23% ($p = 0.040$) significant decrease in motion. During lateral bend loading, unilateral, and bilateral fixations, respectively, resulted in a 51% ± 23% ($p = 0.004$) and 51% ± 16% ($p = 0.001$) significant decrease in ROM. During axial rotation loading, unilateral, and bilateral fixations, resulted in 32% ± 14% ($p = 0.008$) and 40% ± 17% ($p = 0.010$) significant decreases in ROM, respectively.

The plane center of the instantaneous axis of rotation (cIAR) results upon fixation are shown in Figure 5. Average plane cIAR was calculated during flexion/extension loading in the sagittal plane. The cIAR results also depict the distance (mm) of the cIARs at the intact, unilateral, and bilateral fixed states from the graft implantation site. The intact cIAR was in the cephalad region of the joint, in the region of the posterior superior iliac spine. The graft was implanted at the center of the joint across the articular and fibroid regions. The cIAR upon unilateral fixation was shifted downwards towards the graft implantation site. The cIAR upon bilateral fixation was also located at the center of the joint across articular and fibrous region. During intact testing, the average cIAR was 31 ± 23 mm from the graft placement. Upon unilateral fixation, the average cIAR was 19 ± 25 mm from the graft

Table 1 Outcome Measures Defined to Analyze the Mobility of the Sacroiliac Joint. Relative Motions and Centers of Rotation are Described

Measure	Description & Calculation
Total Rotation in Three Planes	Total angular rotation of sacrum between extents of loading in each of the three planes. Calculated as the Pythagorean sum[a] of rotations on and off of the loading plane.
Coupled Motion Ratio in Three Planes	The percent of angular rotation that occurs in each of the three loading planes. Calculated as the on-axis angular rotation of the sacrum divided by the total angular rotation of the sacrum.
Instantaneous Axis of Rotation (IAR) in Sagittal Plane	The helical instantaneous axes mapped out by the centrodes about which the sacrum rotates relative to the ilium. To calculate the IARs, lines were made connecting the positions of every combination of sacrum perimeter markers with their subsequent positions between each 1.5 Nm loading interval instances, in both directions, which produced an adequate amount of on-axis angular separation (~0.1°).28 Perpendicular bisectors were then extrapolated from these and the intercepts located the centrodes (C) which defined the helical IAR. C1: 0 Nm to +1.5 Nm C2: +1.5 Nm to + 3 Nm C3: +3 Nm to +4.5 Nm C4: +4.5 Nm to +6 Nm C5: +6 Nm to +7.5 Nm C6: −6 Nm to −7.5 Nm C7: −4.5 Nm to −6 Nm C8: −3 Nm to −4.5 Nm C9: −1.5 Nm to −3 Nm C10: 0 Nm to −1.5 Nm
Center of the Instantaneous Axis of Rotation in Flexion and Extension Directions (Direction cIAR)	Linear axis which passes through the center of the helical instantaneous axes of rotation, projected unto the joint's sagittal plane as a point, between extents of loading in flexion and extension directions of motion. Calculated as the average location of the centrodes, which define the helical instantaneous axes of rotation of the sacrum over ten loading intervals[b].
Center of the Instantaneous Axes of Plane Rotation (Plane cIAR)	Linear axis which passes through the center of the helical instantaneous axes of rotation, projected unto the joint's anatomic loading plane as a point, between extents of loading in the sagittal plane of motion. Calculated as the average location of the directional cIAR which constituted motion in the sagittal plane[c]. Sagittal Plane: Flexion (+ve) and Extension (-ve) cIARs

Notes: [a]The Pythagorean sum of a set of numbers x_1, x_2, …, x_n is defined as $\sqrt{x_1^2 + x_2^2 + \ldots + x_n^2}$. [b]The negative (-ve) and positive (+ve) Direction cIARs for a set of centrodes defining the IAR are defined as $cIAR_{Flex} = \frac{C_1+C_2+C_3+C_4+C_5}{5}$, $cIAR_{Ext} = \frac{C_6+C_7+C_8+C_9+C_{10}}{5}$. [c]The Plane cIARs for a set of positive and negative directions are defined as $cIAR_{FE} = \frac{cIAR_{Flex} + cIAR_{Ext}}{2}$.

implantation site, and upon bilateral fixation, the average cIAR was 10 ± 3 mm from the graft implantation site. Unilateral and bilateral fixation, respectively, resulted in a 53% ± 26% ($p = 0.047$) and 51% ± 32% ($p = 0.050$) reduction in the distance of the cIAR from the graft's implantation site.

Correlation analysis of ROM and cIAR results are shown in Figure 6. Upon fixation, change in the flexion/extension cIAR had a moderate linear (R^2=0.5279, $p \leq 0.0292$) correlation with the percent reduction in total ROM during flexion-extension loading.

Discussion

The goal of this study was to characterize changes in sacroiliac joint biomechanics upon posterior intra-articular fixation of the joint. From the results obtained, posterior unilateral and bilateral fixations of the sacroiliac joint were able to significantly reduce the total range of motion during flexion-extension, lateral bending, and axial rotation motions. We also conclude that the posterior fixation is effective in shifting the center of the instantaneous axis of rotation (cIAR), to the allograft's location, and this shift may be an indicator of increased joint-allograft

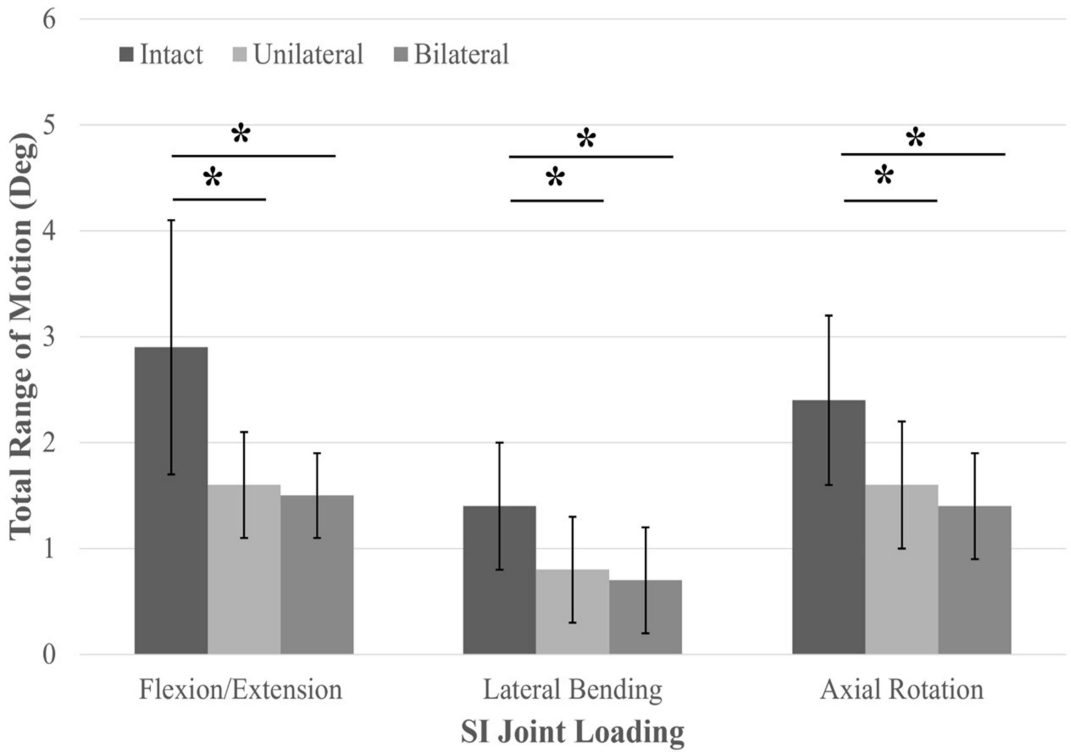

Loading		Flexion/Extension Plane			Lateral Bending Plane			Axial Rotation Plane		
Test Condition		*Intact*	*Unilateral*	*Bilateral*	*Intact*	*Unilateral*	*Bilateral*	*Intact*	*Unilateral*	*Bilateral*
A Right	F	4.1	1.1	1.1	1.5	0.7	0.5	2.4	1.3	1.0
A Left		4.2	1.8	1.5	1.7	0.5	0.6	2.0	1.5	0.9
B Right	F	1.2	1.2	1.0	0.6	0.2	0.3	1.2	0.7	0.9
B Left		1.7	1.3	1.4	1.0	0.7	0.4	3.6	2.3	1.8
C Right	M	2.9	2.2	2.0	1.9	1.6	1.2	2.6	2.4	2.2
C Left		3.2	2.2	2.1	2.0	0.9	1.4	2.2	1.4	1.5
Mean ± Stdev **Total Range of Motion**		**2.9 ± 1.2**	**1.6 ± 0.5***	**1.5 ± 0.4***	**1.4 ± 0.6**	**0.8 ± 0.5***	**0.7 ± 0.5***	**2.4 ± 0.8**	**1.6 ± 0.5***	**1.4 ± 0.5***
Mean ± Stdev **Coupled Motion Ratio** (100% * On-Axis Rotation/Total Rotation)		**82.2 ± 16.3**	**90.1 ± 9.5**	**96.0 ± 3.2**	**64.3 ± 36.9**	**68.6 ± 38.6**	**73.7 ± 20.5**	**84.2 ± 11.7**	**85.5 ± 6.1**	**85.7 ± 5.6**

Figure 4 Ranges of rotational motion in three planes. The x-axis lists the three planes of loading. The y-axis displays the total rotation in each direction and plane of motion. The asterisk (*) indicates statistically significant reductions in flexion-extension, lateral bending, and axial rotation motions from the intact condition. The table shown lists the numbers used to create the chart and the coupled motion ratio. All data are represented as mean ± standard deviation. A, B, C represent individual donors from which sacroiliac joints were obtained.

coupling complex stability, resulting in little or no micromotion at the location of the graft. The elimination of micromotion at the implantation site is an important precedent for improved fusion outcomes at the implant, as well as the reduced incidence of pseudoarthrosis.[29–31] Furthermore, we conclude that this shift in the plane center of the Instantaneous Axis of Rotation (cIAR) towards the graft implantation site upon fixation is moderately and positively correlated with the increased reduction in the total range of motion (ROM) during flexion/extension loading (R^2=0.5279, p<0.03). However, moderate correlation cannot confirm causation between outcome measures,

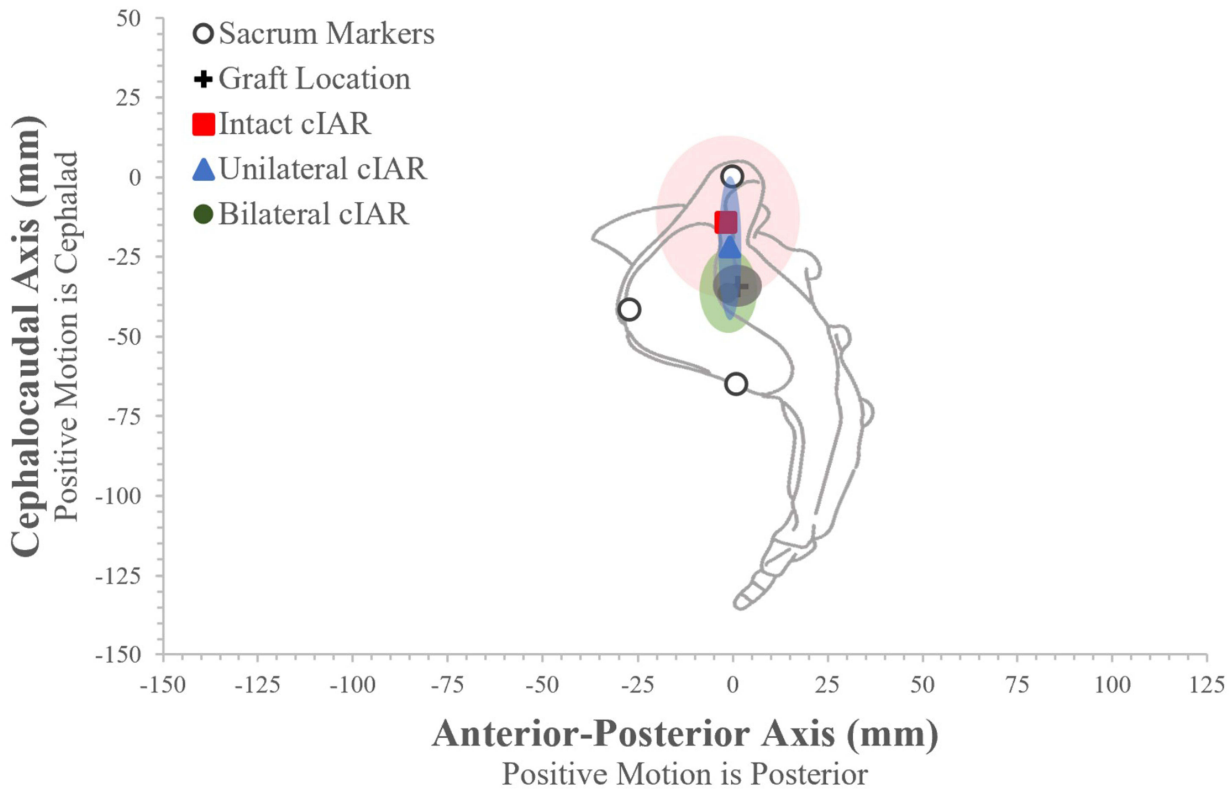

	Anterior Distance (mm)	Caudal Distance (mm)	Distance from Graft Center (mm)
Graft Location	1 ± 6	34 ± 7	0 ± 0
Intact Plane cIAR	-2 ± 19	14 ± 26	31 ± 22
Unilateral Plane cIAR	-1 ± 3	22 ± 23	19 ± 25*
Bilateral cIAR	-1 ± 7	36 ± 13	10 ± 3*

Figure 5 Approximated anatomic view of the sacrum overlaid on the normalized sacral markings (white). The origin is set as the sacral perimeter mark representing the superior end of the ala. The normalized cIARs between the extents of flexion/extension loading are displayed on the left lateral sacrum. All data are represented as means with standard deviations highlighted in ellipses. Light red ellipse is the standard deviation for the intact cIAR. Dark grey ellipse is the standard deviation for the graft location. Light blue ellipse is the standard deviation for the unilateral cIAR. Light green ellipse is the standard deviation for the bilateral cIAR. The asterisk (*) in the table, indicates statistically significant difference in the distance of the cIAR from the graft's location, during the intact range of motion compared to unilateral and bilateral fixed ranges of motion.

but indicates that both outcomes are coupled in this novel approach.

Our results are corroborated by previous in-vivo and in-vitro investigations of sacroiliac joint biomechanics.[8–13,32–34] We report 2.9 ± 1.2 degrees, 1.4 ± 0.6 degrees, and 2.4 ± 0.8 degrees of intact flexion-extension, lateral bending, and axial rotation loading. Previous investigations have reported 2.3 ± 1.4 degrees to 4.5 ± 3.3 degrees for flexion/extension loading, 1.1 ± 0.8 degrees to 1.5 ± 1.5 degrees for during left/right lateral bending, and 1.7 ± 0.8 degrees to 2.9 ± 2.1 degrees during left/right axial rotation.[8–13] We also report that the center of the instantaneous axis of rotation (cIAR) during intact flexion-extension, is in the cephalad region of the joint, in the region of the posterior superior iliac spine. This is in agreement with previous investigations of the sacroiliac joint's Instantaneous Axes of Rotation, which have also placed the flexion-extension instantaneous axis of rotation (IAR) posterior to the joint and in the region of the iliac tuberosity.[32–34] The coupled motion ratios observed for flexion/extension, left/right lateral bending, and left/right axial rotation loads were 82% ± 16%, 64% ± 37%, and 84% ± 12%, respectively;

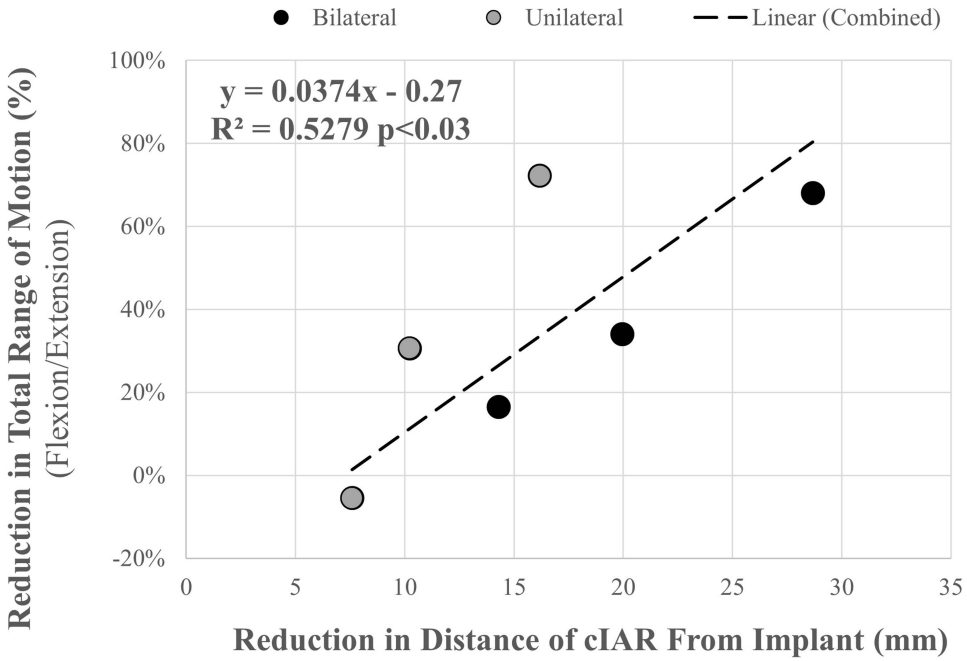

Figure 6 Scatter Plot and Correlation Analysis of outcome measures. The x-axis displays the percentage reduction in the distance of the cIAR from the implant. The y-axis displays the percentage reduction in total range of rotational motion during flexion/extension loading. The correlation coefficient (R^2) indicates a moderate relationship between outcome measures, with equation shown above.

Odeh et al reported ratios of 96% ± 5%, 61% ± 30%, and 95% ± 6% for the same pure moment loads. Identical coupled motion ratios are observed between flexion/extension, left/right lateral bending, and left/right axial rotation.[35]

We undertook this study within the context of the standard multidirectional bending flexibility model with pure-moment load application, which has been utilized by many investigations of spinal fusion techniques because of its consistency and reliability.[36,37] Optical markers were placed near the tested sacroiliac joint to guarantee that bone deformation during asymmetrical loading did not influence the range of motion results.[38] Still, our study is not without limitations. The pure-moment flexibility loading scheme may not accurately represent typical in-vivo loading. Pure moments are correlated with in vivo motions in single planes, such as flexion during rise-to-stand, rotation, and bending during gait and positioning during activities of daily living. They do not match the complexity of combined multiplanar in-vivo loading. All specimens were of good bone quality, and further studies would be required to determine the effect of osteopenia and osteoporosis on fixation performance. While the amount of motion reduction required to promote fusion is not known, previous investigators utilizing triangular rods for lateral sacroiliac fixation, in a similar experimental setup have reported ~34% (unilateral) and ~50% (bilateral) mean reduction in flexion/extension pooled range of motion only.[10] In our investigation, we report ~45% (unilateral) and ~48% (bilateral) reduction for the same mean flexion/extension pooled range of motion, and this is in addition to further reductions in lateral bending and axial rotation motion planes. The current model also cannot simulate biological changes over time. However, the long-term efficacy and safety of this novel fusion allograft in-vivo have been previously demonstrated.[39] Only a fraction of the body mass was applied to the joints through the S1 vertebrae, to avoid limiting the motion of the sacroiliac joint, as cadaveric tissue is stiffer than in vivo.[8–13] However, we were able to replicate results from previous in vivo and in vitro studies.[32–34] Also, it has been shown that variations between small and large compressive loads do not affect the trends in knee joint mobility.[40] Application of the results from the presented model to the clinical scenario should be undertaken with these limitations in mind.

Conclusion

The stabilizing effect on the total range of motion and center of instantaneous axis of rotation in the posterior approach to sacroiliac joint arthrodesis had not been previously quantified or investigated. Our study concludes

that our novel posterior approach presents a multifaceted mechanism for stabilizing the joint. The first mechanism of stabilization is presented by the reduction of the total range of motion in all planes of motion, ie, during flexion-extension, lateral bending, and axial rotation. As in-vivo motions are a complex combination of various loads, fixation in all motion planes may result in increased efficacy. A second mechanism of stabilization is presented by shifting the center of the instantaneous axis of rotation (cIAR) towards the implant's location in the predominant plane of motion, ensuring little or no micromotion at the implantation site, thus promoting fusion in this region. Thus, the potential efficacy of this novel approach may be dependent on the accurate positioning of the allograft. While previous investigators have reported efficacy of 66.5% to 76.5% in pain reported outcomes for this approach, there are currently no studies that clinically examine the consistency of the allograft placement.[39,41]

Ethics Approval and Informed Consent

The Western Institutional Review Board (WIRB) found that this research [Confirmation ID: 45002187] is exempt from IRB review because it does not meet the definition of human subject as defined in 45 CFR 46.102. Specifically, investigator is not conducting research to obtain information or biospecimens from living individuals. WIRB has approved the following locations to be used in the research: Medical Device Development, 2255 Hayes Street, San Francisco, California, 94117.

Acknowledgments

The authors acknowledge Rhea Lamba and Jason Goetting from Medical Device Development, Inc. for their work in specimen testing and data processing.

Funding

This study was funded by PainTEQ Inc. Test implant and instrumentation were provided by PainTEQ Inc.

Disclosure

Dr Dawood Sayed and Dr Ramana K Naidu report stock options from PainTeq. Dr Steven Falowski reports personal fees, equity, and/or consultant and research from CornerLoc, PainTeq, and Aurora, outside the submitted work. The authors report no other conflicts of interest in this work.

References

1. Hartvigsen J, Hancock MJ, Kongsted A, et al. What low back pain is and why we need to pay attention. *Lancet*. 2018;391(10137):2356–2367. doi:10.1016/S0140-6736(18)30480-X
2. Falowski S, Sayed D, Pope J, et al. A review and algorithm in the diagnosis and treatment of sacroiliac joint pain. *J Pain Res*. 2020;13:3337–3348. doi:10.2147/JPR.S279390
3. Bernard TN Jr, Kirkaldy-Willis WH. Recognizing specific characteristics of nonspecific low back pain. *Clin Orthop Relat Res*. 1987;1(217):266–280.
4. Schwarzer AC, Aprill CN, Bogduk N. The sacroiliac joint in chronic low back pain. *Spine*. 1995;20(1):31–37. doi:10.1097/00007632-199501000-00007
5. Maigne JY, Aivaliklis A, Pfefer F. Results of sacroiliac joint double block and value of sacroiliac pain provocation tests in 54 patients with low back pain. *Spine*. 1996;21(16):1889–1892. doi:10.1097/00007632-199608150-00012
6. Smith-Petersen MN. Arthrodesis of the sacroiliac joint: a new method of approach. *JBJS*. 1921;8(3):400–405.
7. Smith-Petersen MN, Rogers WA. End-result study of the arthrodesis of the sacroiliac joint for arthritis - traumatic and non-traumatic. *JBJS*. 1926;1(8):118–136.
8. Lindsey DP, Perez-Orribo L, Rodriguez-Martinez N, et al. Evaluation of a minimally invasive procedure for sacroiliac joint fusion - an in vitro biomechanical analysis of initial and cycled properties. *Med Devices*. 2014;7:131–137. doi:10.2147/MDER.S63499
9. Soriano-Baron H, Lindsey DP, Rodriguez-Martinez N, et al. The effect of implant placement on sacroiliac joint range of motion: posterior versus transarticular. *Spine*. 2015;40(9):E525–E530. doi:10.1097/BRS.0000000000000839
10. Lindsey DP, Parrish R, Gundanna M, Leasure J, Yerby SA, Kondrashov D. Biomechanics of unilateral and bilateral sacroiliac joint stabilization: laboratory investigation. *J Neurosurg Spine*. 2018;28(3):326–332. doi:10.3171/2017.7.SPINE17499
11. Jeong JH, Leasure JM, Park J. Assessment of biomechanical changes after sacroiliac joint fusion by application of the 3-dimensional motion analysis technique. *World Neurosurg*. 2018;117:e538–e543. doi:10.1016/j.wneu.2018.06.072
12. Shih YC, Beaubien BP, Chen Q, Sembrano JN. Biomechanical evaluation of sacroiliac joint fixation with decortication. *Spine J*. 2018;18(7):1241–1249. doi:10.1016/j.spinee.2018.02.016
13. Cross WW, Berven SH, Slater N, Lehrman JN, Newcomb AGUS, Kelly BP. In vitro biomechanical evaluation of a novel, minimally invasive, sacroiliac joint fixation device. *Int J Spine Surg*. 2018;12(5):587–594. doi:10.14444/5072
14. Endres S, Ludwig E. Outcome of distraction interference arthrodesis of the sacroiliac joint for sacroiliac arthritis. *Indian J Orthop*. 2013;47(5):437–442. doi:10.4103/0019-5413.118197
15. Stark JG, Meyer CL, Brown GA, et al. Fusion of the sacroiliac joint: new technique and functional outcome. Conference Proceedings American Academy of Orthopaedic Surgeons Annual Meeting; San Francisco, USA; February 2008.
16. Polly DW Jr. The sacroiliac joint. *Neurosurg Clin N Am*. 2017;28(3):301–312. doi:10.1016/j.nec.2017.03.003
17. Stark J, Fuentes J, Fuentes T, et al. The history of sacroiliac joint arthrodesis: a critical review and introduction of a new technique. *Curr Orthop Pract*. 2011;22(6):545–557. doi:10.1097/BCO.0b013e31823563d3
18. Venayre B, Koyama Y, Kurosawa D, et al. Quantitative evaluation of the sacroiliac joint fixation in stress reduction on both sacroiliac joint cartilage and ligaments: a finite element analysis. *Clin Biomech*. 2021;85:105350. doi:10.1016/j.clinbiomech.2021.105350
19. Thongtrangan I, Balabhadra RS, Kim DH. Management of strut graft failure in anterior cervical spine surgery. *Neurosurg Focus*. 2003;15(3):E4. doi:10.3171/foc.2003.15.3.4

20. Mesbah M, Barkaoui A. Biomechanical investigation of the effect of pedicle-based hybrid stabilization constructs: a finite element study. *Proc Inst Mech Eng H*. 2020;234(9):931–941. doi:10.1177/0954411920934956
21. Daftari TK, Chinthakunta SR, Ingalhalikar A, Gudipally M, Hussain M, Khalil S. Kinematics of a selectively constrained radiolucent anterior lumbar disc: comparisons to hybrid and circumferential fusion. *Clin Biomech*. 2012;27(8):759–765. doi:10.1016/j.clinbiomech.2012.05.010
22. Yang SW, Langrana NA, Lee CK. Biomechanics of lumbosacral spinal fusion in combined compression-torsion loads. *Spine*. 1986;11(9):937–941. doi:10.1097/00007632-198611000-00014
23. Perez-Orribo L, Zucherman JF, Hsu KY, Reyes PM, Rodriguez-Martinez NG, Crawford NR. Biomechanics of a posterior lumbar motion stabilizing device: in vitro comparison to intact and fused conditions. *Spine*. 2016;41(2):E55–E63. doi:10.1097/BRS.0000000000001148
24. Dar G, Peleg S, Masharawi Y, et al. Sacroiliac joint bridging: demographical and anatomical aspects. *Spine*. 2005;30(15):E429–E432. doi:10.1097/01.brs.0000172232.32082.e0
25. Herrington L. Assessment of the degree of pelvic tilt within a normal asymptomatic population. *Man Ther*. 2011;16(6):646–648. doi:10.1016/j.math.2011.04.006
26. States RA, Pappas E. Precision and repeatability of the Optotrak 3020 motion measurement system. *J Med Eng Technol*. 2006;30(1):11–16. doi:10.1080/03091900512331304556
27. Eguizabal J, Tufaga M, Scheer JK, Ames C, Lotz JC, Buckley JM. Pure moment testing for spinal biomechanics applications: fixed versus sliding ring cable-driven test designs. *J Biomech*. 2010;43(7):1422–1425. doi:10.1016/j.jbiomech.2010.02.004
28. Crawford N. Technical Note: Determining and displaying the instantaneous axis of rotation of the spine. *World Spine J*. 2006;1:53–56.
29. Riew KD, Yang JJ, Chang DG, et al. What is the most accurate radiographic criterion to determine anterior cervical fusion? *Spine J*. 2019;19(3):469–475. doi:10.1016/j.spinee.2018.07.003
30. Lee NJ, Vulapalli M, Park P, et al. Does screw length for primary two-level ACDF influence pseudoarthrosis risk? *Spine J*. 2020;20(11):1752–1760. doi:10.1016/j.spinee.2020.07.002
31. Thomé C, Krauss JK, Zevgaridis D. A prospective clinical comparison of rectangular titanium cages and iliac crest autografts in anterior cervical discectomy and fusion. *Neurosurg Rev*. 2004;27(1):34–41. doi:10.1007/s10143-003-0297-2
32. Egund N, Olsson TH, Schmid H, Selvik G. Movements in the sacroiliac joints demonstrated with roentgen stereophotogrammetry. *Acta Radiol Diagn*. 1978;19(5):833–846. doi:10.1177/028418517801900513
33. Jacob HA, Kissling RO. The mobility of the sacroiliac joints in healthy volunteers between 20 and 50 years of age. *Clin Biomech*. 1995;10(7):352–361. doi:10.1016/0268-0033(95)00003-4
34. Brunner C, Kissling R, Jacob HA. The effects of morphology and histopathologic findings on the mobility of the sacroiliac joint. *Spine*. 1991;16(9):1111–1117. doi:10.1097/00007632-199109000-00017
35. Odeh K, Wu W, Taylor B, Leasure J, Kondrashov D. In-vitro 3D analysis of sacroiliac joint kinematics: primary and coupled motions. *Spine*. 2021;46(8):E467–E473. doi:10.1097/BRS.0000000000003841
36. Fuller AM, Chui JM, Cook DJ, Yeager MS, Gladowski DA, Cheng BC. Verification of pure moment testing in a multi-degree of freedom spine testing apparatus. *Int J Spine Surg*. 2012;6(1):1–7. doi:10.1016/j.ijsp.2011.12.001
37. Wheeler DJ, Freeman AL, Ellingson AM, et al. Inter-laboratory variability in in vitro spinal segment flexibility testing. *J Biomech*. 2011;44(13):2383–2387. doi:10.1016/j.jbiomech.2011.06.034
38. Pool-Goudzwaard A, Gnat R, Spoor K. Deformation of the innominate bone and mobility of the pubic symphysis during asymmetric moment application to the pelvis. *Man Ther*. 2012;17(1):66–70. doi:10.1016/j.math.2011.09.002
39. Sayed D, Balter K, Pyles S, Lam CM. A multicenter retrospective analysis of the long-term efficacy and safety of a novel posterior sacroiliac fusion device. *J Pain Res*. 2021;14:3251–3258. doi:10.2147/JPR.S326827
40. Müller O, Lo J, Wünschel M, Obloh C, Wülker N. Simulation of force loaded knee movement in a newly developed in vitro knee simulator. *Biomed Tech (Berl)*. 2009;54(3):142–149. doi:10.1515/BMT.2009.015
41. Deer TR, Rupp A, Budwany R, et al. Pain relief salvage with a novel minimally invasive posterior sacroiliac joint fusion device in patients with previously implanted pain devices and therapies. *J Pain Res*. 2021;14:2709–2715. doi:10.2147/JPR.S325059